2022 年【全國科學探究競賽-這樣教我就懂】

大專/社會組 科學文章表單

文章題目：Bifunctional plasma-induce biomass-derived graphene quantum dot(GQD)-polymer composite for water purification and quality self-monitoring

文章內容：（限 500 字~1,500 字）

Abstract

我們提出使用生質能甲殼素經過綠色電漿製程，不須加入任何還原劑，並在大氣常壓穩定進行電化學反應，生成高經濟價值石磨烯量子點(GQD)。石墨烯量子點 結合的薄膜納米複合材料 (TFN) 膜，該膜具有增強的透水性。由於體積小、分散穩定和官能團活性，GQDs 在哌嗪（PIP）和均苯三甲酰氯（TMC）的界面聚合過程中以一種簡便的方式嵌入到聚酰胺（PA）層中。通過傅里葉變換紅外 (FTIR) 光譜、X 射線光電子能譜 (XPS)、水接觸角、zeta 電位、掃描電子顯微鏡 (SEM) 和原子力顯微鏡 (AFM) 對所得 TFN 膜的表面化學特徵和形貌進行表徵） 測量。隨著 GQDs 含量的增加，TFN 膜的表面粗糙度降低，TFN 膜的表面親水性增強。根據納濾（NF）實驗，TFN 膜的最高水通量在 0.2 MPa 的操作壓力下達到 336.0 L/(m2 h)，是原始 PA 膜的近 24 倍。除此之外，我們開發一種新型感測技術，可同時偵測薄膜阻塞(低於五微米)，此技術為薄膜檢測注入了新的靈魂。

Introduction

For the past few years, freshwater scarcity poses great threat to the sustainable development of human society. Membrane technologies, including nanofiltration (NF) and reverse osmosis (RO), have found increasing applications in water purification and reclamation. Thin film composite (TFC) membranes consisting of an ultrathin polyamide (PA) layer, are the most widely used NF and RO membranes. However, due to the inherent limitations of conventional TFC membranes, the preparation of a TFC membrane with a high flux while maintaining a good rejection is still a challenging task.[1]

In recent years, considerable efforts have been devoted to explore the advanced thin film nanocomposite (TFN) membranes. It has been found that the water fluxes and antifouling properties of the TFN membranes improved remarkably through the appropriate introduction of nanoparticles into PA layers. However, subject to the poor dispersibility and compatibility of some nanoparticles in PA layers, there still exists a large room for the elevation of the membrane performance. Nowadays, carbon materials have been widely used in sensing, electromagnetic interference (EMI) shielding, photocatalysts and functional materials, because of its superior properties of electronic, mechanical, optical, and transparent nature. In some studies, carbon materials such as carbon nanotubes (CNTs) and graphene oxide (GO) nanosheets, were

incorporated into the PA layers during interfacial polymerization. The obtained TFN membranes integrated the advantages of both polymer materials and carbon materials.

Generally, NGQDs synthesis methods are classified into two major types including direct synthesis using top-down or bottom-up technologies and post-growth doping.However, special precursors and chemicals, long reaction time, and laborious preparation procedures are required. Synthesis of NGQDs by post-growth doping usually requires a long reaction time to treat the mixtures of nitrogen precursors and pre-synthesized GQDs under high temperature. Overall, it is still lacking a simple, scalable, and environmental-friendly method to synthesize NGQDs with well controlled structures.[3]

Very recently, graphene quantum dots (GQDs), which share most of the excellent features of GO, have emerged in broad application fields such as catalysis, bioimaging, lighting, sensing, biological label, optoelectronic and energy. Futhermore, we conjectured that the synthetic GQDs with a smaller size (~2 nm) and higher crystallinity may be utilized in fabricating TFN membranes with high water fluxes and antifouling properties. Overall, it is still lacking a simple, scalable, and environmental-friendly method to synthesize NGQDs with well-controlled structures.[4]

Here **we reported a direct synthesis of NGQDs under ambient conditions using chitosan as the sole carbon and nitrogen precursor by atmospheric-pressure microplasmas. During the synthesis, no strong acid or toxic chemicals were additionally used.** However, TFN membranes incorporated with GQDs were fabricated via interfacial polymerization of piperazine (PIP) and trimesoyl chloride (TMC) with GQDs as aqueous additives. The influence of the GQDs addition on surface morphology, hydrophilicity and charge density was investigated in detail. Separation and antifouling performance of the resultant TFN membranes was evaluated by using NF experiments. **This study may present a useful attempt to the fabrication of TFN membranes with high flux and antifouling properties towards high-efficient water treatment and achieve a new method for self-monitoring dye-cake formation.**

Figure 1. Schematic of microplasma-enable fabricated biomass-derived NGQD/PA for muti-application.

Results and Discussion

A microplasma synthesis of diameter-controlled colloidal graphene quantum dots under ambient conditions is demonstrated. UV-Visible absorption spectroscopy was used to identify the optical absorption of various electronic states present in the synthesized NGQDs. Figure 2(a) shows the UV-Visible absorbance spectra of the samples synthesized with 9.6 mA current and time for 60min. The absorption bands shown suggest the existence of various electronic states in the as-synthesized NGQDs. The highest absorption of each spectrum at 281 nm is attributed to $\pi \rightarrow \pi^*$ transitions of C=C structures and may also due to $n \rightarrow \pi^*$ transitions of C−N bonds.. However, MicroRaman characterization was performed to study the vibrational structures of chitosan and NGQDs (Figure 2(b)). Chitosan shows a broad G-band at 1571 cm−1 due to its amorphous structures, while the NGQDs exhibit not only a sharp G-band at 1598 cm−1, referring to high crystalline graphene structure, but also the D-band of NGQDs located at 1348 cm−1 originated from structural disorder in the graphene lattice caused by N-dopant, vacancy due to non-graphitic N-doping, and edges. As a consequence, the averaged intensity ratio of the D-band and G-band (ID/IG) was calculated to be 1.02 ± 0.06, indicating the disordered carbon atom and yet highly crystalline. This result is close to what has been reported by Kumar et al., which further confirms that the NGQDs contain a large number of defects in the form of edges and surface functional groups. Moreover, NGQDs show no observable Raman peak above 1600 cm^{-1}, unlike chitosan. This result indicates that **the purification is successful and can increase the practicability of NGQDs.** TEM was performed to study the morphologies of the synthesized NGQDs. The TEM image presented in Figure 2(c) shows particle-like nanostructures with no aggregation and amorphous coating observed. The fast Fourier transform (FFT) image in the inset reveals the crystalline structure of NGQDs. The lattice spacing of 0.24 nm can be confirmed through high-resolution TEM (HRTEM), indicating (1120) lattice fringes of graphene. Overall, the above results suggest that **our method provides a simple and environmental-friendly method to synthesize photo luminescent NGQDs under ambient conditions using microplasmas.**

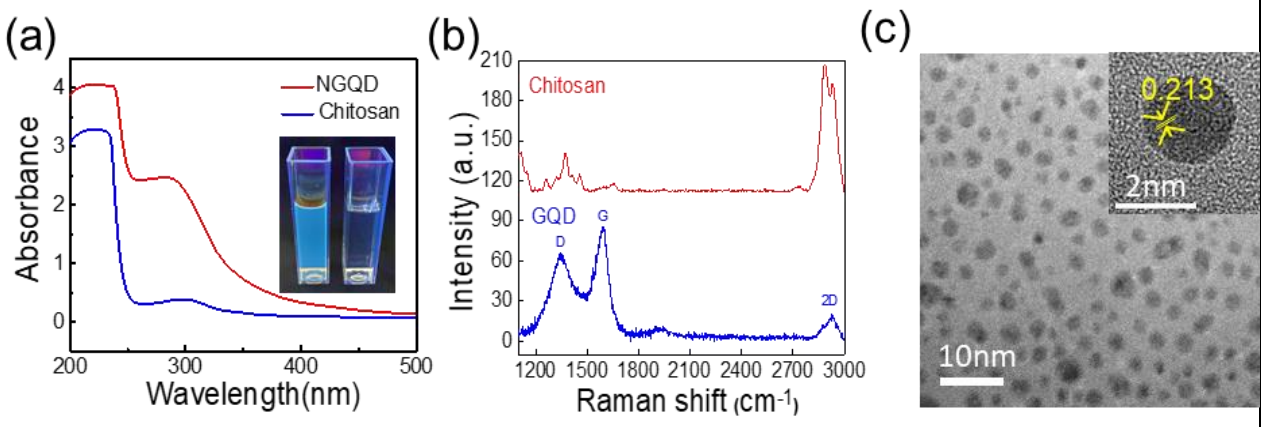

Figure 2.(a) Schematics of experimental setup for NGQD synthesis using a microplasma reactor. (b) MicroRaman spectra of chitosan and NGQDs. The NGQDs were synthesized by a microplasma at 9.6 mA discharge current for 60-min.(d) HRTEM image with a lattice spacing of NGQDs

The influence of GQDs on the surface morphology of the resultant TFN membranes was characterized by SEM. As can be seen from Fig. 3(a,b), the PIP-TMC NF membrane has a dense and rugged surface. This was caused by the fast reaction rate of the interfacial polymerization between PIP and TMC. However, the GQDs/PIPTMC TFN membranes have relatively flower-like structure membrane surfaces. This was because the incorporation of GQDs may bind with PIP or TMC and lower cross-linking reaction rate. It has been proved that lower crosslinking reaction rates and stronger intermolecular hydrogen bonding interactions can result in the formation of flower-like nodular structures on membrane surfaces. The hydrophilicity of the membrane surfaces was evaluated by the static water contact angle measurement. In general, lower water contact angle represents higher hydrophilicity of surface. As shown in Fig. 3(c), with the increase of GQDs content from 0 to 1.0 wt%, the water contact angle continuously decreased from 74.0° of the PIP-TMC NF membrane to 17.0° of the GQDs/PIP-TMC TFN membrane, which could be understood from the surface chemical properties and the surface microstructures. On one hand, the introduction of GQDs determined the extent of surface functionalization by carboxyl and hydroxyl groups and the change of surface microstructures; On the other hand, the incorporation of GQDs promoted the formation of water channel structures, which would affect the wettability of membrane surfaces. [5]

NF performance of the GQDs/PIP-TMC TFN membranes was tested, as shown in Fig. 3. The water flux of the PIP-TMC NF membrane was only 15.0 L/(m^2 h), which was relatively lower because of the dense PA layer. With the GQDs added, the hydrophilicity of the membrane surfaces enhanced. **The incorporation of GQDs led to the formation of more water channels within the PA layer, which was beneficial for water to pass through.[6] The water flux of the GQDs/PIP-**

TMC TFN membrane dramatically increased to 273 L/(m^2 h), which was 19 times higher than that of the pristine PIP-TMC NF membrane.

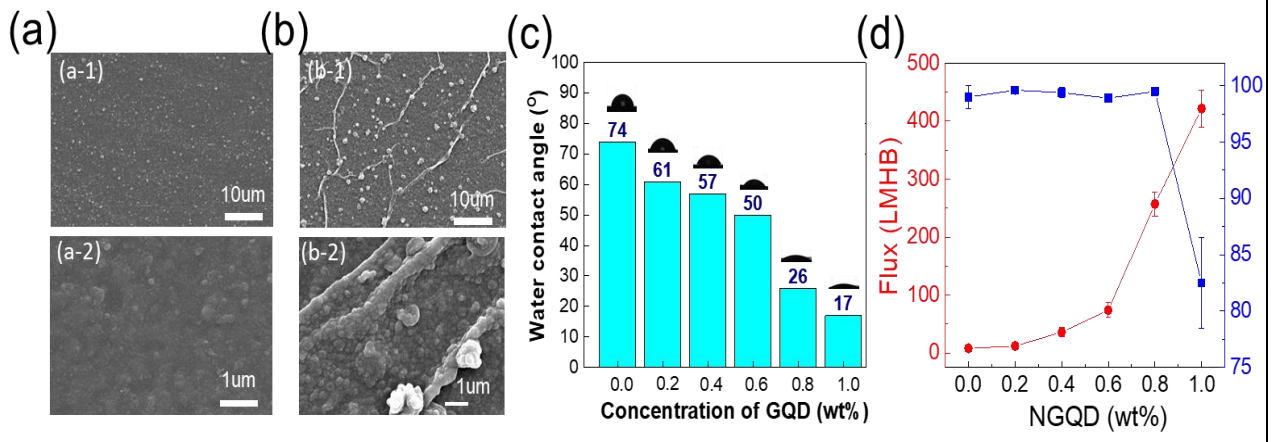

Figure. 3. SEM Image of pristine PA (a) and 0.8% GQD/PA (b). (c) water contact angles of the PIP-TMC NF membrane and the GQDs/PIP-TMC TFN membranes with different GQDs contents. (d) Water fluxes (a) and rejections to dye (b) of the PIP-TMC NF membrane and the GQDs/PIP-TMC TFN membranes with different GQDs contents under operation pressure of 0.2 MPa. Each above value was based on the average of two independent membranes fabricated under the same condition.

Because GQDs are the zero-dimensional material and quantum confinement effect. In addition, Figure 4(a) shows a contour plot of the obtained PL intensity as a function of excitation and emission. The obtained map shows one maximum in PL intensity (shown in red) with 360 and 420 nm of excitation and emission, respectively, which represents a radiative recombination center. Following the time for filtration application, the dye-cake is covered by the surface of GQD membrane. This induced the PL intensity to decrease dependent on the filtering time. However, the recyclability performance of various NF composite membranes, including GQD MF membranes , in dye filtration was further compared in Fig. 4(b). When other NF composite membranes in recent reports are evaluated[7], our as-prepared GQD membrane has a superior permeation flux and a lower flux decay by the time. **Interestingly, we could also detect dye-cake formation using the PL method when the long-term test. By PL method, we achieve the fouling detection below 5 um. It's the fantastic results to overcome the world record.**

Figure 4. (a) PL spectrum for self-monitoring dependent filtration time (b) Nanofiltration

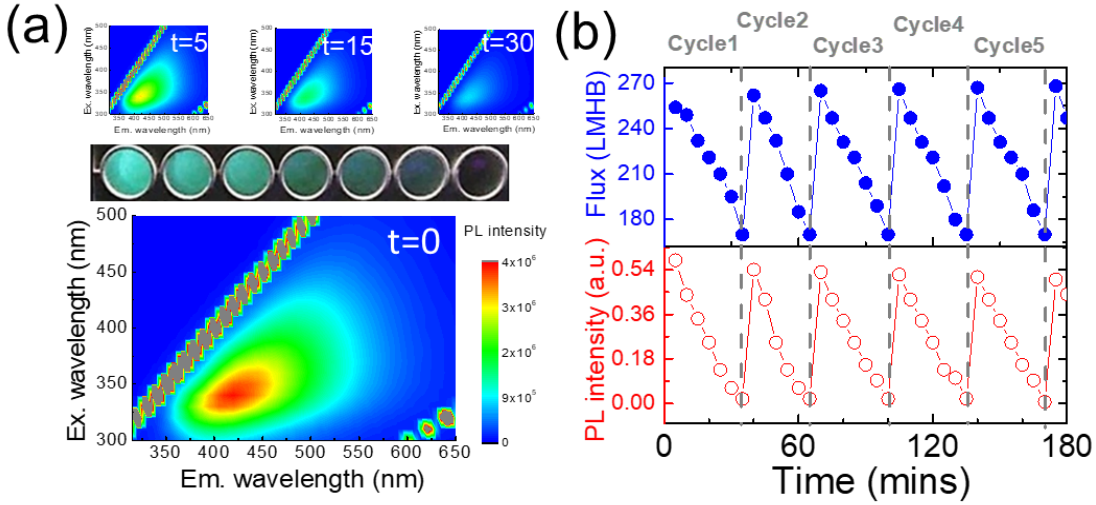

performance and self –monitoring recovery of the GQD membrane

參考資料

1. Marchetti, P., et al., Molecular separation with organic solvent nanofiltration: a critical review. Chemical reviews, 2014. 114(21): p. 10735-10806.
2. Aravind, J., Graphene: Important Results and Applications. 2020, Springer.
3. Chen, W., et al., Synthesis and applications of graphene quantum dots: a review. Nanotechnology Reviews, 2018. 7(2): p. 157-185.
4. Ponomarenko, L.A., et al., Chaotic Dirac billiard in graphene quantum dots. Science, 2008.
5. Dou, H., et al., Analogous Mixed Matrix Membranes with Self-Assembled Interface Pathways. Angewandte Chemie International Edition, 2021. 60(11): p. 5864-5870.
6. Lecaros, R.L.G., et al., Alcohol dehydration performance of pervaporation composite membranes with reduced graphene oxide and graphene quantum dots homostructured

filler. Carbon, 2020. 162: p. 318-327.
7. Tang, X., et al., The role of electrostatic potential polarization in the translocation of graphene quantum dots across membranes. Nanoscale, 2020. 12(4): p. 2732-2739.

註：

1. 沒按照本競賽官網提供「表單」格式投稿，不予錄取。
2. 建議格式如下
   - 中文字型：微軟正黑體；英文、阿拉伯數字字型：Times New Roman
   - 字體：12pt 為原則，若有需要，圖、表及附錄內的文字、數字得略小於 12pt，不得低於 10pt
   - 字體行距，以固定行高 20 點為原則